Journal of Volcanology and Geothermal Research 302 (2015) 24–32

Contents lists available at ScienceDirect

Journal of Volcanology and Geothermal Research

journal homepage: www.elsevier.com/locate/jvolgeores

Explosive volcanic activity at Mt. Yasur: A characterization of the acoustic events (9–12th July 2011)

Laura Spina [a,b,*], Jacopo Taddeucci [c], Andrea Cannata [d], Stefano Gresta [a,c], Luigi Lodato [d], Eugenio Privitera [d], Piergiorgio Scarlato [c], Mario Gaeta [e], Damien Gaudin [c], Danilo Mauro Palladino [e]

[a] Dipartimento di Scienze Biologiche, Geologiche ed Ambientali, Sezione Scienze della Terra, Università di Catania, Corso Italia 57, Catania 95129, Italy
[b] Department für Geo- und Umweltwissenschaften, Sektion für Mineralogie, Petrologie und Geochemie, Ludwig-Maximilians-Universität München, Theresienstr. 41, 80333, München, Germany
[c] Istituto Nazionale di Geofisica e Vulcanologia, Via Di Vigna Murata 605, 00143, Roma, Italy
[d] Istituto Nazionale di Geofisica e Vulcanologia, Osservatorio Etneo, Sezione di Catania, Piazza Roma 2, 95123, Catania, Italy
[e] Dipartimento di Scienze della Terra, Sapienza-Università di Roma, Piazzale Aldo Moro, 5, 00185 Roma, Italy

ARTICLE INFO

Article history:
Received 13 January 2015
Accepted 9 June 2015
Available online 14 June 2015

Keywords:
Acoustic events
Mt. Yasur
Degassing activity
Thermal analyses

ABSTRACT

Volcanic processes occur in a wide range of temporal and spatial scales. However, a key step of magma ascent is recognizable in the dynamics of gas and magma in the shallow plumbing system, where volatiles play a fundamental role in controlling the eruptive style. With the aim of investigating shallow degassing processes, an experimental setup was deployed at Mt. Yasur, an active volcano located in Tanna Island (Vanuatu arc), from 9th to 12th July 2011. The setup comprised high-speed and thermal cameras, as well as a microphone, capable of recording both in the infrasonic and audible range. The analysis of acoustic signals, validated by observing images from the high-speed and thermal cameras, has enabled characterizing the explosive activity during the investigated period. Two types of explosions, distinct for spectral features and waveforms, were observed: (i) minor events, corresponding to small overpressurized bursts, occurring almost continuously; (ii) major events, characterizing the Strombolian activity at Mt. Yasur. By investigating variation in the occurrence rate of the minor events, we found that, on a short timescale, the dynamics responsible for the two types of explosions are decoupled. These results, together with previous literature data, bring additional evidence of the existence of distinct sources of degassing. Finally, major events can be distinguished as emergent events, i.e. long-lasting signals, corresponding to ash-rich explosions, and impulsive events, featuring shorter duration and larger amplitude.

1. Introduction

Mt. Yasur is a basaltic-andesitic volcano, in the archipelago of Vanuatu, Southwest Pacific Ocean. It is located in the central part of the New Hebrides Island Arc, 150 km above the Benioff plane (Carney and Macfarlane, 1979; Louat et al., 1998) related to the subduction of the Indo-Australian Plate below the Pacific Plate. It is a relatively small volcano (361 m a.s.l. high, 1500 m diameter; Fig. 1), constantly active at least since the first report in 1774 (Aubert de la Rüe, 1960; Peltier et al., 2012). Volcanic activity has been occurring at Mt. Yasur since 1400 years BP (e.g. Métrich et al., 2011). There are three active vents at the summit area, aligned in a NE-SW direction and commonly referred to as vents A, B and C (from south to north; e.g. Oppenheimer et al., 2006). They are the source of open vent degassing and recurrent explosions, propelling hot gases and magma fragments a few hundred meters above the craters (Nabyl et al., 1997; Oppenheimer et al., 2006; Bani et al., 2013).

One of the most relevant features of Mt. Yasur volcano is the persistence of Strombolian explosive activity, which has characterized the volcano's eruptive style for at least 800 years (McClelland et al., 1989), being only sporadically interrupted by sub-Plinian explosive phases (Nairn et al., 1988). Huge variations in the number of the explosions (up to a factor of 5) and acoustic pressure (up to a factor of 4) were observed by means of year-long recordings performed with a microbarometer (Zielinski et al., 2010). The switching between different degassing regimes was linked to either sudden or slow variations of the gas fraction in the conduit (Zielinski et al., 2010). A notable variability in the intensity and number of explosions was also reported during February–July 2003, when the daily number of explosions ranged between 20 and 1300 (Le Pichon et al., 2005). Therefore, many attempts to describe the dynamics of the explosive behavior of Mt. Yasur have been done. Recently, Marchetti et al. (2013) interpreted the infrasonic events recorded at Mt. Yasur in July/August 2008 as blast waves produced by violent Strombolian

* Corresponding author at: Department für Geo- und Umweltwissenschaften, Sektion für Mineralogie, Petrologie und Geochemie, Ludwig-Maximilians-Universität München, Theresienstr. 41, 80333, München, Germany. Tel.: +49 89 2180 4218; fax: +49 89 2180 4176.
E-mail address: laura.spina@min.uni-muenchen.de (L. Spina).

http://dx.doi.org/10.1016/j.jvolgeores.2015.06.005
0377-0273/

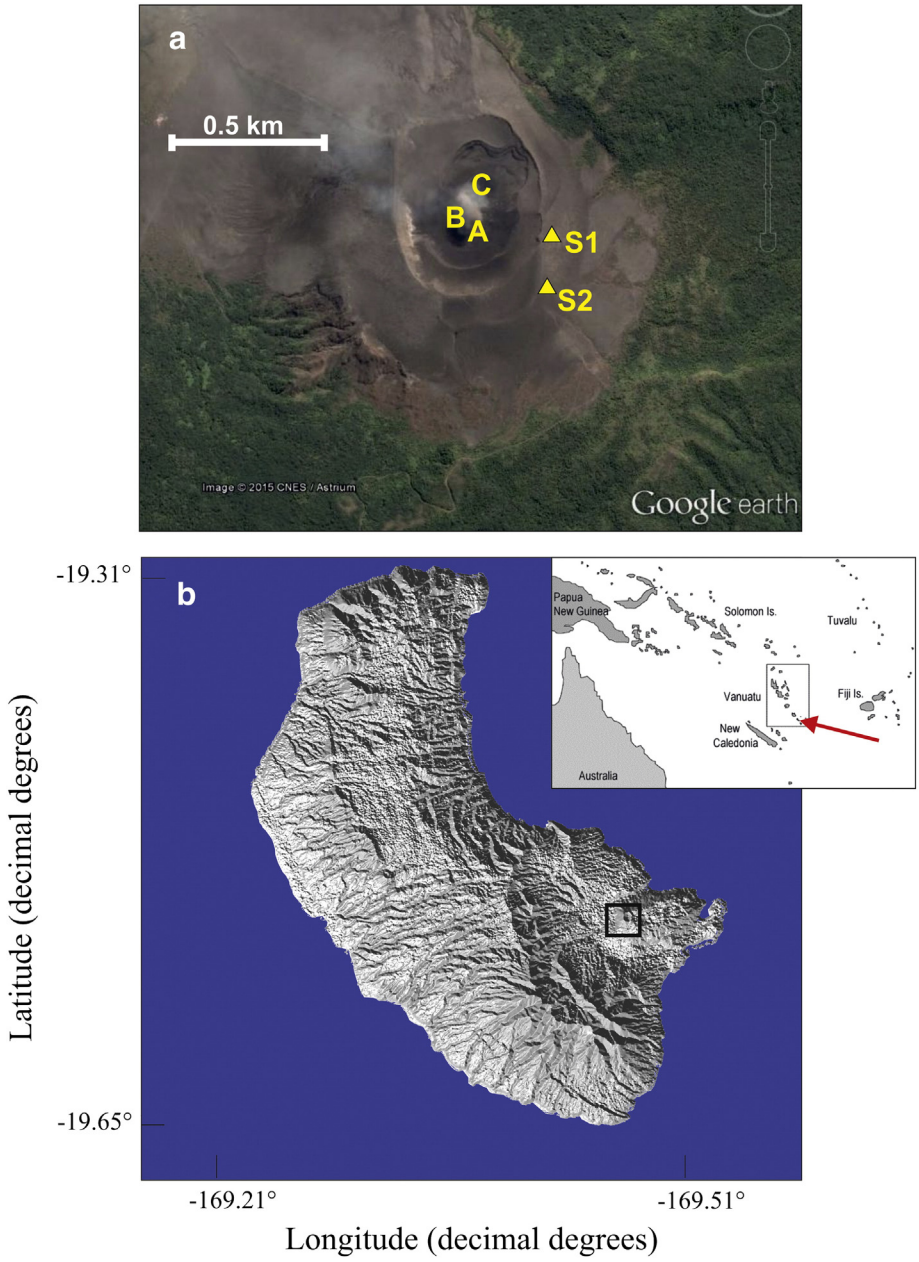

Fig. 1. (a) Satellite image of the Mt. Yasur summit area (©2014 Google Data SIO, NOAA, U.S. Navy, NGA, GEBCO; Image ©2015 CNES/Astrium). The position of the main active vents are indicated by the letters A, B, C, while the recording sites are indicated by S1 (Site 1) and S2 (Site 2). (b) Digital elevation model of Tanna Island. The black rectangle indicates the location of Mt. Yasur. In the top inset, the location of Vanuatu arc is shown; the red arrow marks the position of Tanna Island.

activity driven by supersonic dynamics. Bani et al. (2013), based on the thermal energy of individual explosions, defined two groups of bursting events. The first comprised the majority of the recorded events (up to 87%), exhibiting low energy values. The remaining part of the dataset was made up of a smaller number (13%) of high-energy explosions. The absence of any correlations between the two types of explosions led them to infer the existence of two different source dynamics. The occurrence of a two-scale dynamics was also suggested by the FTIR spectroscopy (Oppenheimer et al., 2006). The authors found higher values ($\approx$30) of SO_2/HCl ratio for high-energy events rather than for passive degassing and small bursting ($\approx$2). This allowed them to infer the existence of a deep source, rich in SO_2 and CO_2, for Strombolian explosions, and a shallow source, enriched in HCl, feeding passive degassing.

In this work, we investigate this dual scale of degassing, as well as the complexity and variability of the explosive activity at Mt. Yasur, through a multiparametric study, performed from 9th to 12th July 2011 (GMT time). The employed setup, called FAMoUS (Fast Multiparametric Setup for Real-time Observations; Freda et al., 2012), includes (1) an Optronis CamRecord 600×2 high-speed camera; (2) a FLIR SC655 thermal camera; (3) an InfraCyrus microphone. The latter has an instrumental response curve of 0 dB (1 V/Pa at 1 KHz) between 20 and 3000 Hz. This microphone also shows a nearly flat response between 1 and 10 Hz. Further details on the instrumental response in the infrasonic range are given in Buonocunto et al. (2011). Signals were acquired with a sampling rate of 10 kHz.

We synchronized the sensors via a hand- or microphone-operated trigger. Due to the high-frequency sample rate used in this study, signals were not acquired continuously. Our dataset therefore consisted of tens of traces lasting from a few to several minutes and collected at intervals from a few to tens of minutes apart.

We elected to focus our attention on vents A and B, and accordingly two locations were alternatively chosen as recording sites for logistical

Table 1
Times and locations of the performed recording phases.

Sampling phase	Day	Recording times (GMT)	Recording site
1	9–10th July	11 p.m. – 1.40 a.m.	Site 1
2	10th July	5.45 – 6.40 a.m.	Site 2
3	11th July	4.45 – 6.13 a.m.	Site 2
4	11–12th July	11.20 p.m. – 1.40 a.m.	Site 1
5	12th July	6.50 – 7.10 a.m.	Site 2

reasons (Table 1). In this paper, they are named Site 1 (S1) and Site 2 (S2) (Fig. 1) and are located at a horizontal distance of 283 and 312 m from Vent A, respectively. In detail, during the evening of 9th and 11th July, the station was placed along the eastern crater rim (Site 1), while on the other days, it was located along the southeastern crater rim of A-B vents (Site 2), about 13 m below its position at Site 1. In the latter, the instrumentation was partially occluded from the crater rim.

On the days preceding our study (7–8th July), a high level of activity with strong degassing and ash emission, accompanied by the observation of fresh volcanic bombs along the crater rim, was reported by the Vanuatu Geohazards Observatory (Global Volcanism Program, 2011). Similarly, throughout the duration of our recording, the activity consisted of spattering and puffing interrupted by more violent Strombolian explosions, ejecting bombs hundreds of meters above the vent.

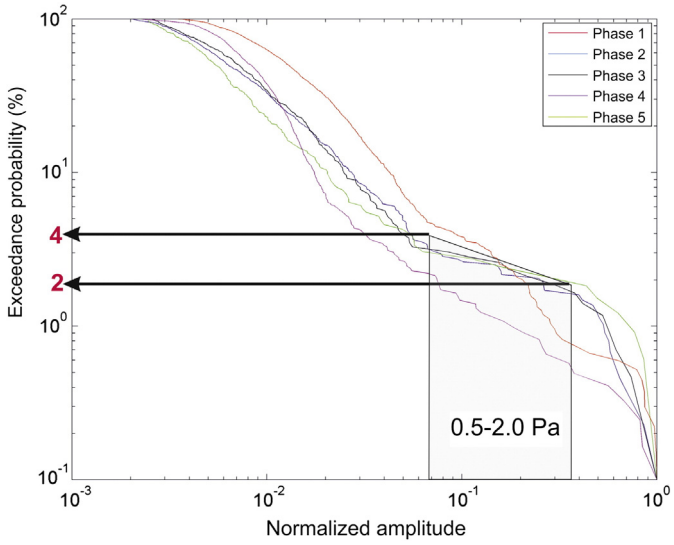

Fig. 3. Exceedance probability distribution of the normalized amplitude of the acoustic events (the phase number refers to the sampling phase as reported in Table 1), respectively. The black arrows mark the range of amplitude values (0.5–2.0 Pa) and corresponding exceedance probability (2%–4%) for which a decrease in the slope of the curve was observed at Site 2 (sampling phases 2, 3, and 5). The values of amplitudes mark the amplitude range separating minor and major events.

2. Data analysis

We computed the root mean square (RMS) of the acoustic traces, using a 0.3 s moving window with a shift of 0.1 s. On the basis of the relative distances between vent A and recording sites, we also determined the reduced RMS values (Fig. 2), which are the equivalent pressures at 1 m from the source (see Johnson et al., 2004; McNutt et al., 2013 for details). Interestingly, a decrease in the reduced RMS amplitude is evident in connection with recordings performed at Site 2 (Fig. 2).

In order to identify and count infrasonic events over the background, a percentile trigger, able to detect transients very close to each other (for details on the method, see Cannata et al., 2011), was applied on the RMS series (Fig. 2). We then calculated the peak-to-peak amplitude of all the detected events, and the corresponding exceedance probability plot (Fig. 3). Since the events were recorded during 5 different recording phases and from 2 different sites, before calculating the exceedance probability, the peak-to-peak amplitudes recorded during each phase were normalized, dividing by the maximum value obtained during the same phase. The exceedance probability plot clearly shows a trend change, separating all the events into 2 distinct populations, i.e. "major events" (2%–4% of all the detected events) and "minor events" (98%–96% of all the detected events).

We looked closely at both event types and characterized them as follows: (i) major events, i.e. strong bursts with a large increase of amplitude with respect to the noise level, with peak-to-peak amplitudes up to 25 Pa and (ii) minor events, associated with amplitudes about ten times smaller (generally <1 Pa), waveforms of 1 to 1.5 cycles, lasting roughly 1 s (Figs. 3 and 4). The regular repetition of such small events characterizes the degassing activity between the occurrences of major events. The observation of synchronized videos from the thermal and the visible high-speed cameras enabled relating the minor and major events,

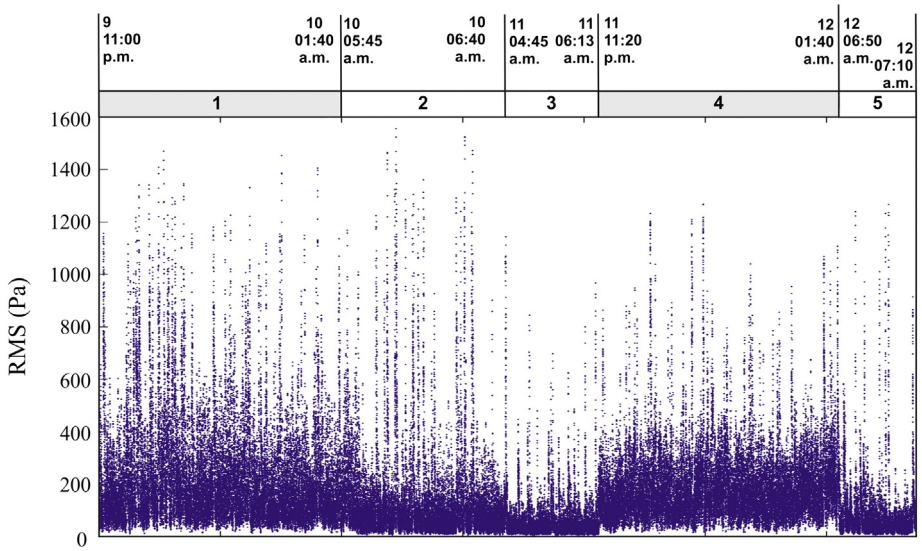

Fig. 2. Plot of RMS series, computed on windows of 0.3 s, with shift of 0.1 s, and reduced at 1 m from the source. The grey and white bars at the top represent periods of recordings performed at S1 or S2, respectively, while the numbers refer to the sampling phases (see also Table 1). The start and end times (dd hh:mm) of each sampling phase is reported at the top of each rectangle.

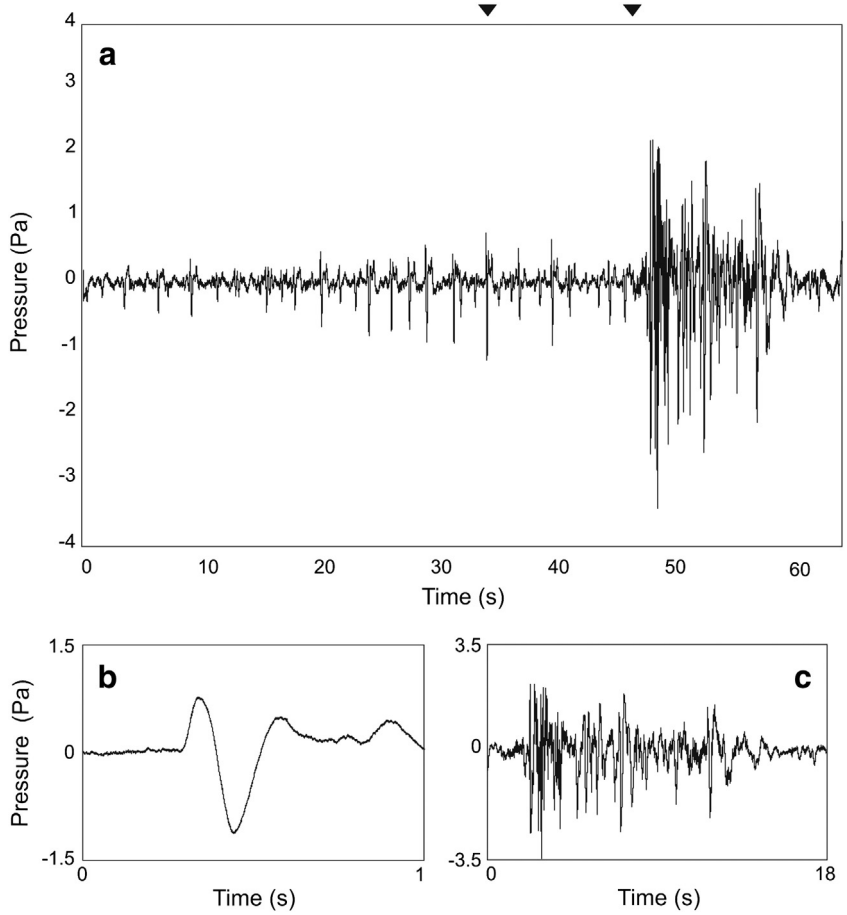

Fig. 4. (a) Example of Mt. Yasur acoustic signals. The time zero in the *x* axis corresponds to July 10th, 06:06:58 (GMT time). The black triangles at the top (a) indicate the time occurrence of a minor event, shown in (b), and of a major explosion, displayed in (c).

respectively, to the almost continuous emission of gas puffs, with occasional pyroclast ejection up to some meters above the vent, and the more violent ejection of ash-bomb mixtures up to hundreds of meters above the vent. Notably, in some cases, major events were characterized by the occurrence of either overlapping or closely spaced bursts. The above differences in the eruptive style are evident from thermal analyses (Fig. 5), where the two types of events, occurring at the same vent, differ up to one order of magnitude in the ejection height of pyroclast as well as in the duration of the emission.

2.1. Minor events

A cross-correlation-based technique has been used to improve the detection of minor events. First, for each signal, we selected a time window containing a representative waveform as template (for instance, see Fig. 4b). The coefficient of cross-correlation between the template and the whole signal was then estimated, by using a moving window with the same length as the template. For the same signals, we selected cross-correlation coefficients with values exceeding the threshold of 0.8. The high threshold ensures that each detection represents a minor event. A total number of almost 5000 minor events were selected from our recordings. Their average rate of occurrence was equal to 40 events/minute. Moreover, the rate of occurrence was also evaluated in relation to the major explosions, to assess the possible existence of a relationship between the two types of events on a short timescale (an example is given in Fig. 6). No meaningful trend or variation in the occurrence rate was found in relation to the arrival of a major event, and therefore, a possible direct and short-term relationship between the two types of events was discarded.

In order to investigate the spectral content of the minor events, a short time Fourier transform was performed using a moving window of 2.56 s with an overlap of 1.28 s (i.e. Figs. 7a, b, and c). Indeed, minor explosions occurred almost persistently during the investigated period. Therefore, we are confident that this kind of continuous-time analysis is able to faithfully represent the spectral features of minor explosions. For the same reason, the peak frequency has also been estimated within the same windows, showing an average value of 1.9 ± 1.0 Hz (Fig. 7d).

2.2. Major events

A total number of 106 major events were collected. For each of them, both peak-to-peak amplitude and duration were estimated. As shown in Fig. 8, the event durations span a wide range of values, between 2 and $\approx$20 s, with an average of 5 s. Peak-to-peak amplitudes are generally comprised between 2 and 25 Pa. Notably, the sampling phases recorded at Site 2 are associated with lower values of amplitudes than at Site 1.

Concerning the spectral features of major events, the bulk of spectral energy is generally below 20 Hz, in the infrasonic range (Fig. 7). However, a variable amount of spectral energy is occasionally present up to roughly 500 Hz.

We observed a high waveform variability in between the major events. We can distinguish between two end-members: (1) impulsive events (Fig. 9a), characterized by a sharp first arrival of the acoustic wave, and (2) emergent events, with slowly increasing amplitude and long codas tapering off (Fig. 9c). Besides first arrival, emergent events usually display longer duration and lower values of amplitude with

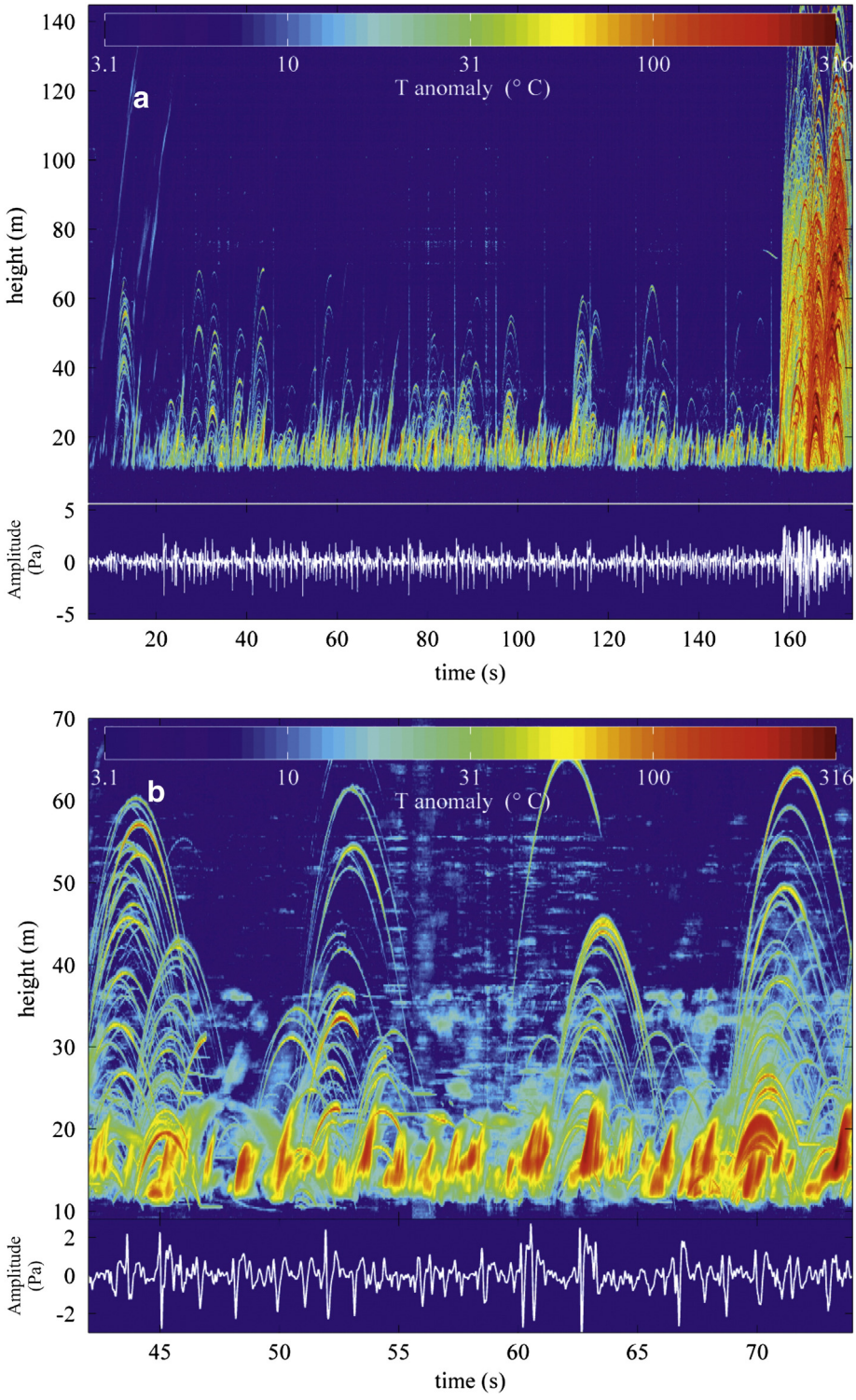

Fig. 5. Characterization of the vent activity from thermal infrared high-speed videos. The temperature anomaly generated by hot gas and pyroclasts is computed for each frame by removing the background temperature, defined for each pixel as the minimum pixel temperature in the 2 s preceding the observation. The time-evolution of the temperature anomaly is represented with respect to the height, by retaining on each frame only the maximum value computed for each row of the video. Gas puffs and bombs appear as streaks and parabolas, respectively, with an inclination related to their rise (or fall) velocity. (a) Multiple small puffs and spatter ejection events and a stronger explosion that ejected bombs higher than the FLIR field of view. (b) Detail of the puffing and spattering.

respect to impulsive ones. Indeed, they represent the totality of the events lasting longer than 12 s in our dataset. As visible in Fig. 8, emergent events were more frequent during the sampling phase 5 (between 12/07 06:50 and 12/07 07:10; Table 1). The comparison with high-speed and thermal videos reveals that impulsive and emergent end-members are both associated with the release of ash and hot bombs from the vents. However, emergent events generally show lower velocity, higher ash fraction and lower apparent temperature of the ash than impulsive ones (Figs. 10b and d). Furthermore, some emergent events showed such low values of acoustic amplitudes to be hardly

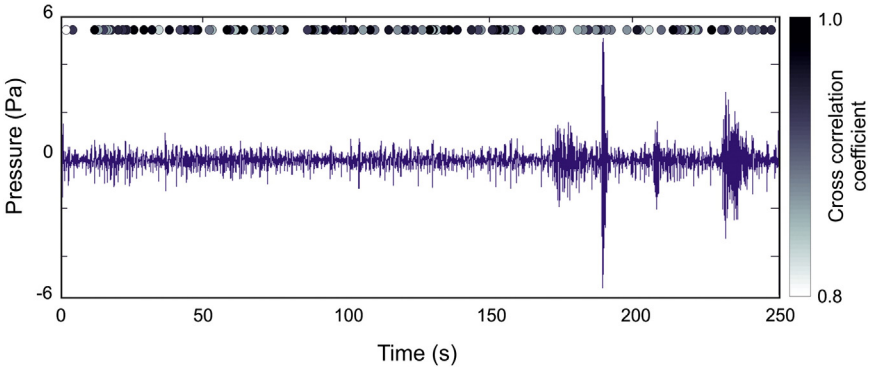

Fig. 6. Acoustic signal, showing 250 s of Mt. Yasur explosive activity. Time zero in the *x* axis corresponds to July 9th, 23:08:09 (GMT time). The dots at the top of the plot represent the computed cross-correlation coefficients, with values exceeding the threshold of 0.8 for the same signal. The color of the dots indicates the value of the cross-correlation coefficient (see the color bar at the left of the figure). Due to the high threshold, each dot represents a detection of a minor event. Note that the rate of occurrence of minor events shows no relation with the occurrence of major ones.

distinguishable from noise or puffing activities. In these cases, thermal and high-speed video images were used to identify them (Fig. 10f).

3. Discussion

3.1. Major versus minor events

Based on the waveform's appearance, amplitude, and spectra, a first general distinction has been made between major and minor events. While the former have rather complex and variable shapes with durations spanning a relatively wide interval (2–20 s) and individual differences in their spectra, the latter are characterized by a high level of self-similarity and steadiness. Coupled analysis of the thermal and video images shows that minor events correspond to small-scale explosions, which eject mainly gas and little/no pyroclasts. This kind of activity, known as "puffing", has previously been identified and characterized at Stromboli (Ripepe et al., 1996, 2007), where a persistent (0.5–1 Hz) and low amplitude (≈1 Pa) signal was associated with the release of hot steam containing droplets and hot ash particles (Harris et al., 2003). Puffing activity has been linked to the degassing of the magma column, occurring in overpressurized conditions, and related to different and decoupled dynamics from the source of Strombolian explosions

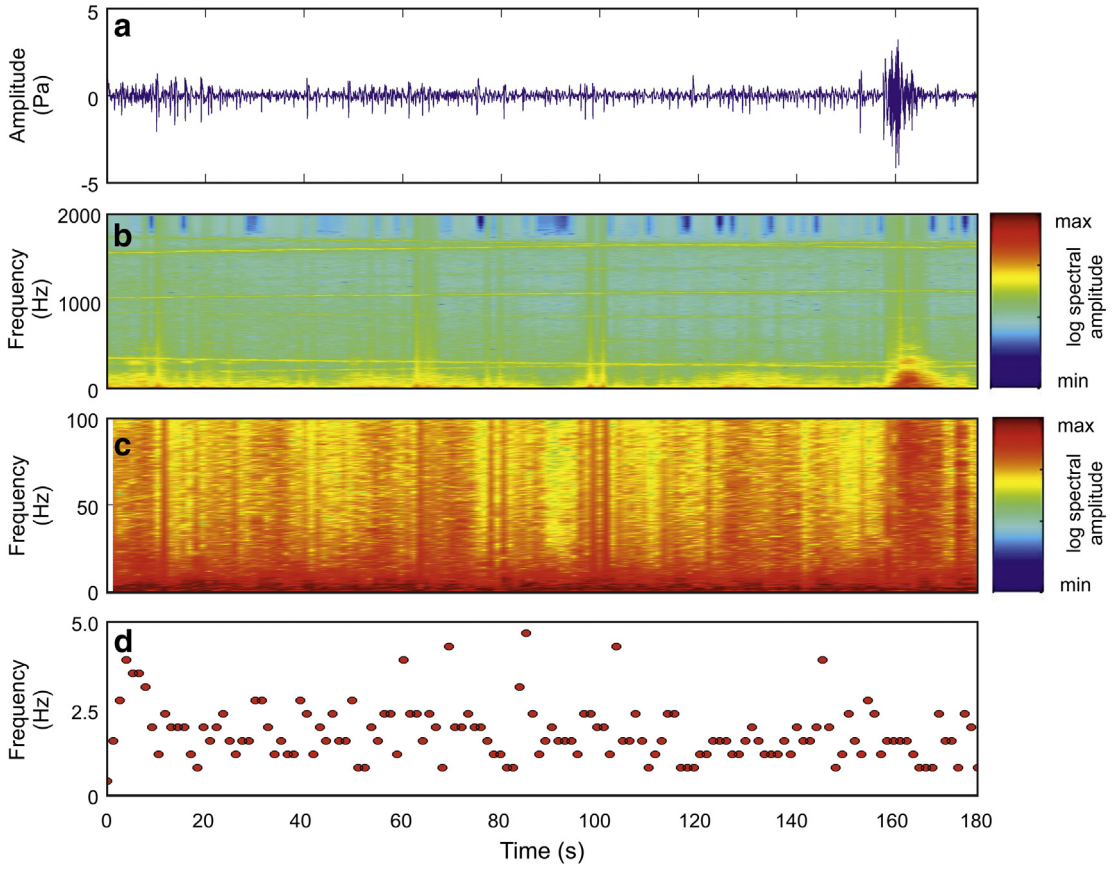

Fig. 7. (a) Acoustic trace, showing ≈170 s of signals. The zero in the timeline corresponds to July 10th, 01:26:29. (b) Normalized spectrogram of the signal performed on a window of 2.56 s with shift of 1.28 s. (c) Detail of (b) in the 0–100 Hz frequency range. (d) Peak frequencies calculated on windows of 2.56 s with shift of 1.28 s. Note that the color bar in (b) and (c) stands for the logarithm of the spectral amplitude.

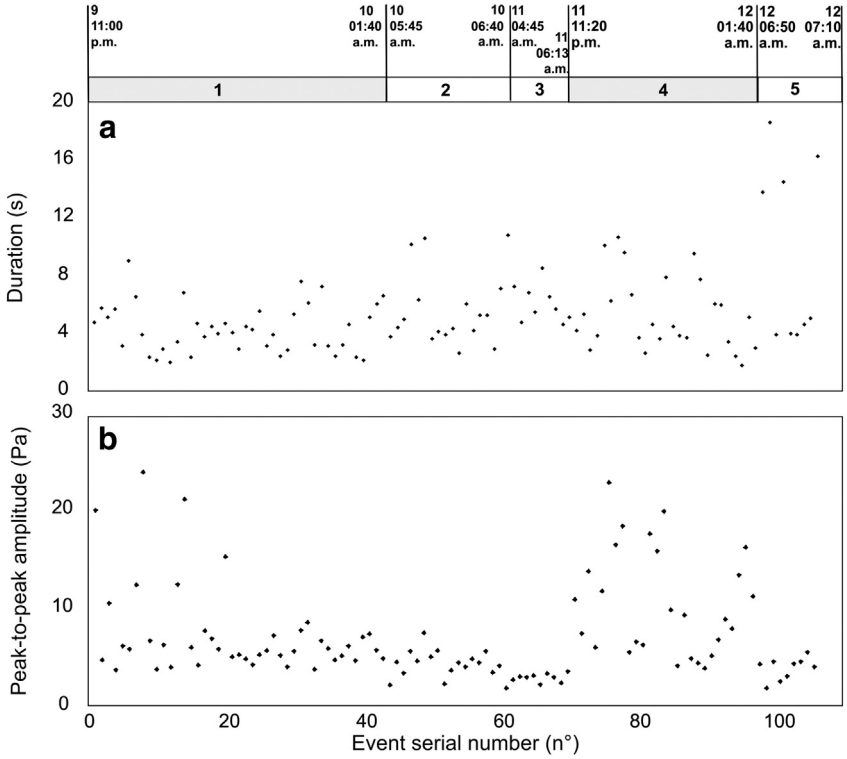

Fig. 8. (a) Duration and (b) peak-to-peak amplitude of the major events. Grey and white bars and numbers at the top of the figure are the same as Fig. 2.

(Ripepe et al., 2007). More recently, Ripepe et al. (2008) observed a correlation between the rate of occurrence of puffing events and Strombolian explosions, suggesting that puffing activity is related to high gas flux regimes in the conduit, and therefore variations in rate, amplitude, and location of puffing reflect changes in the gas flux. It is worth noting that the close similarity between the eruptive dynamics at Stromboli and Mt. Yasur has led several authors to compare them (e.g. Nabyl et al., 1997; Gaudin et al., 2014b). Our results show that the acoustic signature of Mt. Yasur's explosive activity closely resembles the signals previously recorded at Stromboli (Ripepe et al., 1996, 2007), confirming the possible analogy in the degassing dynamics.

As mentioned above, a dual dynamics of degassing at Mt. Yasur was previously observed by FTIR spectrometer measurements (Oppenheimer et al., 2006) and thermal infrared remote sensing (Bani et al., 2013). Our findings are in agreement with the observations of Bani et al. (2013). Using a thermal infrared thermometer, they recorded about 200 explosive events, grouped in high and low-energy events. In particular, the majority of the dataset in Bani et al. (2013) was made up of low-energy events, similar to our observations (minor events constitute 96%–98% of our dataset). Furthermore, both in our study and in Bani et al. (2013), high-energy events (major events) were often characterized by the occurrence of multiple bursts. Consistent with the evidence

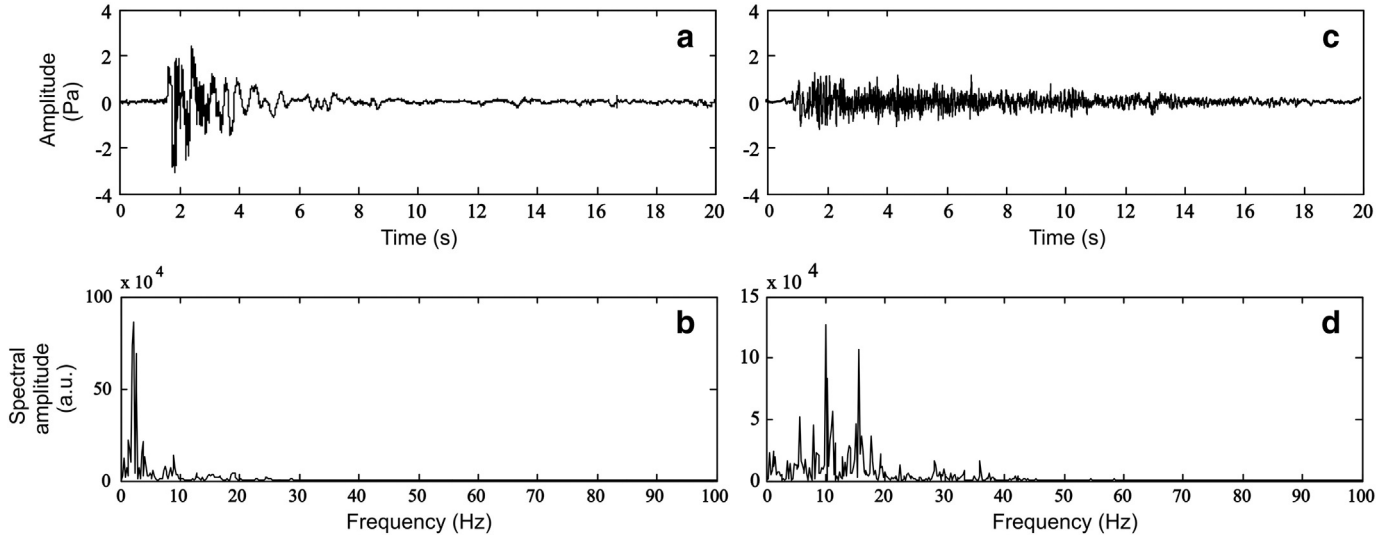

Fig. 9. (a) Example of an impulsive event and (b) related spectrum performed on a window of 5.12 s. (c) Example of an emergent event and (d) related spectrum performed on a window of 5.12 s.

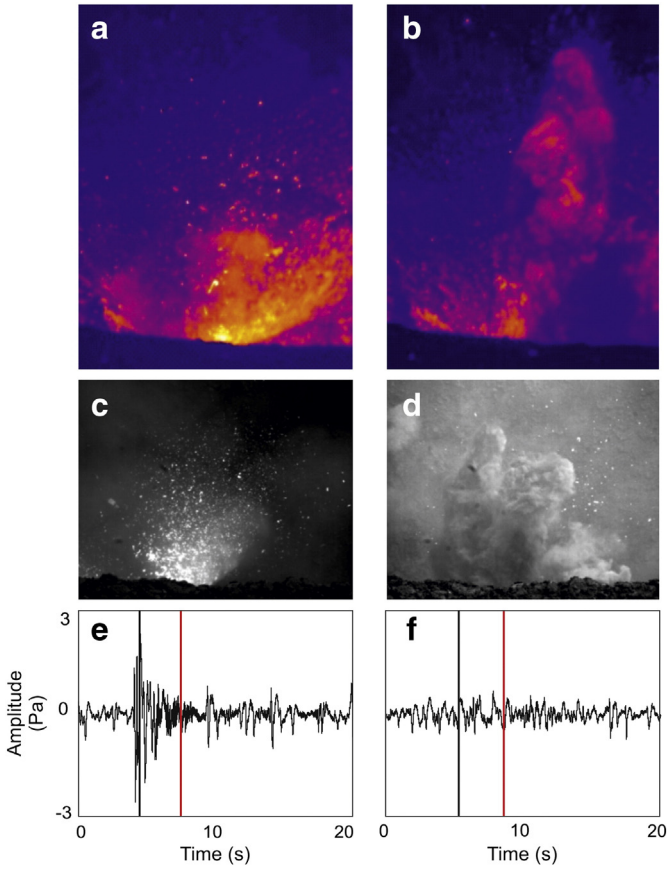

Fig. 10. Examples of two different types of major events, shown by (a,b) still-frame from thermal (in false colors, vertical field of view 138.3 m); (c,d) high-speed video (in grey tones, vertical field of view 35.5 m); and (e,f) acoustic signal; the black and red lines mark the time corresponding to the visible and thermal still frame, respectively. Acoustic traces are time-shifted for travel time from source to receiver. The impulsive event (e) corresponds to a strong explosion with the fast ejection of bombs and relatively hotter ash (a,c). The emergent event (f), with an almost negligible acoustic signal, is associated with a weaker, longer explosion, which ejected bombs and colder ash at lower velocity (b,d).

of different depths of the related sources, inferred from SO_2 and HCl contents (Oppenheimer et al., 2006), a deep and shallow origin was ascribed to high and low-energy events, respectively (Bani et al., 2013).

In the case of Mt. Yasur's acoustic signals, the lack of variation in the rate of minor events before the occurrence of major ones provides no evidence of a direct and immediate relationship between the source dynamics feeding the two activities. The continuity of minor events in time is in agreement with the hypothesis of a continuously active mechanism of generation/release of small pockets of gas, providing magma degassing, whereas the major events can reasonably be linked to cycles of generation-release of more overpressurized slugs at depth. However, we cannot exclude a long-term relationship between the two dynamics, as found by Ripepe et al. (2008) at Stromboli. High-speed video analysis of explosions collected during the period investigated here also shows two distinct classes of events, characterized by differences in the amount and ejection velocity of pyroclasts (Fig. 5; Gaudin et al. 2014a,b).

Finally, it was observed that both RMS and peak-to-peak amplitude computed on the whole dataset (thus including both major and minor events) are systematically lower at Site 2 than Site 1 (see Figs. 2, 3, and 8). This could be related to several possible causes, such as: (i) wind directionality/intensity, (ii) non-monopolar sources, (iii) travel path effects (geometrical spreading, attenuation and scattering, diffraction effects). Despite the lack of quantitative data, wind intensity was qualitatively assessed to be constantly low during the investigated period. Alternatively, the systematic decrease in amplitude at Site 2 may be related to the possible effects of source complexity and directional pattern, due to non-monopole sources (e.g., Johnson et al., 2008). Finally, effects related to the travel path of the acoustic waves in the atmosphere should be considered. Given the small differences in the travel path (≈30 m) between the two sampling sites, dissimilarities in geometrical spreading are negligible, as are anelastic attenuation and scattering in the atmosphere. The observed amplitude differences could however mirror diffraction effects related to the crater rim (Johnson, 2005; Kim and Lees, 2011; Lacanna and Ripepe, 2013). Indeed, Site 2 was partially occluded by the crater rim, which might have acted as an acoustic barrier for the microphone. However, the geometry and characteristics of our setup does not allow discriminating between the above hypotheses.

3.2. Major events: features and dynamics

Mt. Yasur is well renowned for the occurrence of series of Strombolian-mild Vulcanian explosions (i.e. Le Pichon et al., 2005), which in our dataset correspond to the abovementioned major events. A widespread range of acoustic amplitude and rate of occurrence have previously been reported for Mt. Yasur's explosive activity (i.e. Zielinski et al., 2010). Marchetti et al. (2013), for instance, in July/August 2008, at a distance of 700 m from the vents, acoustic events in the range of 5–106 Pa with a rate of up to 60 events/hour and the occurrence of blast waves were recorded. In our study, the acoustic events show peak-to-peak amplitudes up to 25 Pa, measured at ~300 m from the vent, at the lower end of the range reported from Marchetti et al. (2013). Furthermore, while we have no evidence of blast waves in our dataset; a few major events do include jet noise, which has been identified by high-speed videos (Taddeucci et al., 2014).

Based on the arrival of the acoustic waveforms, we distinguished impulsive and emergent major events, similarly to Petersen et al. (2006). The emergent events, generally of longer duration (up to ≈20 s) in the acoustic trace and lower amplitude, were associated in the visual and thermal camera with ash-rich explosions (Fig. 10). Interestingly, Kremers et al. (2013) also recognize two different types of explosions from the seismic and acoustic traces recorded in August–September 2008: the ash-free and the ash-loaded explosions. The emergent events here analyzed are undoubtedly ash-loaded. It is well known that acoustic efficiency of an eruption might be affected by changes in the density-dependent mass transfer and therefore dense ash-rich eruptions are associated with diminished acoustic radiation (i.e. Johnson and Aster, 2005). Nonetheless, in our opinion, the presence of ash is not sufficient by itself to justify their emergent features, since considerable ash contents were involved in some impulsive events. The extended waveform, indeed, may result from a sustained emission of a pyroclastic mixture, as suggested for similar acoustic events at Mt. Augustine (Petersen et al., 2006). In fact, the duration of an explosion has been shown to be a function of the gas overpressure, which directly controls the gas jet velocity (Wilson and Head, 1981; Ripepe and Marchetti, 2002). The emergent explosions can therefore be linked to large volumes of gas arising with lower pressure than impulsive events. However, at Mt. Yasur, Meier et al. (2011) found a strong alteration of the infrasonic signals caused by a fast-moving volcanic cloud and due to Doppler-shifting phenomena. Thus, the influence of the ash and of the temperature of the gas cloud on the infrasonic signals cannot be ruled out, and requires further detailed analyses.

4. Conclusions

In this study, we collected and analyzed the acoustic signal, as well as visible and thermal frames, of Mt. Yasur explosive activity occurring

from 9th to 12th July, 2011. The main outcomes of this research are summarized in the following points.

1. Two types of acoustic events were recognized, based on differences in amplitude, duration, and waveform features. The first, here defined as "minor events", consists of small explosions corresponding to puffing/spattering activity, occurring almost continuously in the analyzed traces. The second type, here named "major events", typifies the Strombolian activity of Mt. Yasur and is linked to more violent explosions that eject ash-bomb mixtures hundreds of meters above the vent. The lack of correlation between the time evolution of these two types of explosions implies that their source dynamics are not directly linked, as also suggested by the clearly separated amplitude distributions.
2. Among major explosions, we distinguished two end-members: (1) impulsive events, generally characterized by short durations and relatively high amplitudes, and (2) emergent events, showing tapered long-lasting waveforms and low amplitudes. Thermal images confirm the involvement of hot pyroclasts in both kinds of explosion. Furthermore, emergent events are generally associated with ash-rich plumes, even though notable amounts of ash were also observed in some impulsive events.

Acknowledgments

We thank M. Ripepe and an anonymous reviewer for their careful review of the manuscript. We are deeply grateful to Carmela Freda for her contribution in collecting data, and to Luca D'Auria and Ciro Buonocunto for assistance in setting up the microphone. We acknowledge the help in the field and support of Esline Garaebiti of the Vanuatu Geohazards Observatory. We thank Stephen Conway for revising and improving the English text.

LS has received support of the European Commission (FP7-MC-ITN, grant number 289976: NEMOH).

This study was supported by MIUR Premiale project North: New hO-Rizons of the Technology applied to experimental researcHes and geophysical and volcanological monitoring.

References

Aubert de la Rüe, E., 1960. Les manifestations actuelles du volcanisme aux Nouvelles Hebrides (Melanesie). Bull. Volcanol. 23, 197–205.

Bani, P., Harris, A.J.L., Shinohara, H., Donnadieu, F., 2013. Magma dynamics feeding Yasur's explosive activity observed using thermal infrared remote sensing. Geophys. Res. Lett. 40, 3830–3835. http://dx.doi.org/10.1002/grl.50722.

Buonocunto, C., D'Auria, L., Caputo, A., Martini, M., Orazi, M., 2011. The InfraCyrus sound sensor. Rapporti tecnici INGV. no 188 (ISSN 2039–7941).

Cannata, A., Montalto, P., Aliotta, M., Cassisi, C., Pulvirenti, A., Privitera, E., Patanè, D., 2011. Clustering of infrasonic events at Mount Etna using pattern recognition techniques. Geophys. J. Int. 185, 253–264. http://dx.doi.org/10.1111/j.1365-246X.2011.04951.x.

Carney, J.N., Macfarlane, A., 1979. Geology of Tanna, Aneityum, Futuna and Aniva. New Hebrides Geological Survey Reportpp. 5–29.

Freda, C., Taddeucci, J., Scarlato, P., Rao, S., Salvaterra, C., Gaeta, M., Palladino, D.M., 2012. The FAMoUS toolbox goes to Yasur: field test of a FAst, MUltiparametric Set-up for real-time observation of explosive eruptions. EGU General Assembly 2012. Geophys. Res. Abstr. Vol. 14 EGU2012-9882.

Gaudin, D., Moroni, M., Taddeucci, J., Scarlato, P., Shindler, L., 2014a. Pyroclast Tracking Velocimetry: A particle tracking velocimetry-based tool for the study of Strombolian explosive eruptions. J. Geophys. Res. Solid Earth 119, 5369–5383. http://dx.doi.org/10.1002/2014JB011095.

Gaudin, D., Taddeucci, J., Scarlato, P., Moroni, M., Freda, C., Gaeta, M., Palladino, D.M., 2014b. Pyroclast Tracking Velocimetry illuminates bomb ejection and explosion dynamics at Stromboli (Italy) and Yasur (Vanuatu) volcanoes. J. Geophys. Res. Solid Earth 119, 5384–5397. http://dx.doi.org/10.1002/2014JB011096.

Global Volcanism Program, 2011. Report on Yasur (Vanuatu). In: Wunderman, R. (Ed.), Bull. Global Network 36:5. http://dx.doi.org/10.5479/si.GVP.BGVN201105-257100.

Harris, A., Johnson, J., Horton, K., Garbeil, H., Ramm, H., Pilger, E., Flynn, L., Mouginis-Mark, P., Pirie, D., Donegan, S., Rothery, D., Ripepe, M., Marchetti, E., 2003. Ground-based infrared monitoring provides new tool for remote tracking of volcanic activity. Eos Trans. AGU 84 (40), 409.

Johnson, J.B., 2005. Source location variability and volcanic vent mapping with a small-aperture infrasound array at Stromboli Volcano, Italy. B. Volcanol. 67, 1–14. http://dx.doi.org/10.1007/s00445-004-0356-8.

Johnson, J.B., Aster, R.C., 2005. Relative partitioning of acoustic and seismic energy during Strombolian eruptions. J. Volcanol. Geotherm. Res. 148, 334–354. http://dx.doi.org/10.1016/j.jvolgeores.2005.05.002.

Johnson, J.B., Aster, R.C., Kyle, P.R., 2004. Volcanic eruptions observed with infrasound. Geophys. Res. Lett. 31, L14604. http://dx.doi.org/10.1029/2004GL020020.

Johnson, J.B., Aster, R., Jones, K., Kyle, P., McIntosh, W., 2008. Acoustic source characterization of impulsive Strombolian eruptions from the Mount Erebus lava lake. J. Volcanol. Geotherm. Res. 177, 673–686.

Kim, K., Lees, J.M., 2011. Finite-difference time-domain modeling of transient infrasonic wavefields excited by volcanic explosions. Geophys. Res. Lett. 38. http://dx.doi.org/10.1029/2010GL046615 (L06804).

Kremers, S., Wassermann, J., Meier, K., Pelties, C., van Driel, M., Vasseur, J., Hort, M., 2013. Inverting the Source Mechanism of Strombolian Explosions at Mt. Yasur, Vanuatu, using a Multi-Parameter Dataset. J. Volcanol. Geotherm. Res. 262, 104–122. http://dx.doi.org/10.1016/j.jvolgeores.2013.06.007.

Lacanna, G., Ripepe, M., 2013. Influence of near-source volcano topography on the acoustic wavefield and implication for source modeling. J. Volcanol. Geotherm. Res. 250, 9–18. http://dx.doi.org/10.1016/j.jvolgeores.2012.10.005.

Le Pichon, A., Blanc, E., Drob, D., Lambotte, S., Dessa, J.X., Lardy, M., Bani, P., Vergniolle, S., 2005. Infrasound monitoring of volcanoes to probe high-altitude winds. J. Geophys. Res. 110. http://dx.doi.org/10.1029/2004JD005587 (D13106).

Louat, R., Hamburger, M., Monzier, M., 1998. Shallow and intermediate depth seismicity in the New Hebrides Arc: Constraints on subduction process. In: Green, H.G., Wong, F.L. (Eds.), Geology and Offshore Resources of Pacific Island Arcs-Vanuatu Region. Earth Sci. Ser. 8. Circum Pacific Council for Energy and Mineral Resources, Houston, Tx, pp. 329–356.

Marchetti, E., Ripepe, M., Delle Donne, D., Genco, R., Finizola, A., Garaebiti, E., 2013. Blast waves from violent explosive activity at Yasur volcano, Vanuatu. Geophys. Res. Lett. 40, 5838–5843. http://dx.doi.org/10.1002/2013GL057900.

McClelland, L., Simkin, T., Summers, M., Nielsen, E., Stein, T.C., 1989. Global Volcanism: 1975–1985. Prentice-Hall, Upper Saddle River, N. J.

McNutt, S.R., Thompson, G., West, M.E., Fee, D., Stihler, S., Clark, E., 2013. Local seismic and infrasound observations of the 2009 explosive eruptions of Redoubt Volcano, Alaska. J. Volcanol. Geotherm. Res. 259, 63–76. http://dx.doi.org/10.1016/j.jvolgeores.2013.03.016.

Meier, K., Hort, M., Tessmer, E., Wassermann, J., 2011. An integrated geophysical approach: Field and modelling studies for a better understanding of infrasound signals at Yasur volcano, Vanuatu. Geophys. Res. Abstr. 13, EGU2011–EGU7852.

Metrich, N., Allard, P., Aiuppa, A., Bani, P., Bertagnini, A., Shinohara, H., Parello, F., Di Muro, A., Garaebiti, E., Belhadj, O., Massare, D., 2011. Magma and Volatile Supply to Post-collapse Volcanism and Block Resurgence in Siwi Caldera (Tanna Island, Vanuatu Arc). J. Petrol. 52 (6), 1077–1105. http://dx.doi.org/10.1093/petrology/egr019.

Nabyl, A., Dorel, J., Lardi, M., 1997. A comparative study of low frequency seismic signals recorded at Stromboli volcano, Italy, and at Yasur volcano, Vanuatu. N. Z. J. Geol. Geophys. 40, 549–558.

Nairn, I.A., Scott, B.J., Giggenbach, W.F., 1988. Yasur volcano investigations, Vanuatu. New Zealand Geological Survey. Department of Scientific and Industrial Research, pp. 1–74.

Oppenheimer, C., Bani, P., Calkins, J.A., Burton, M.R., Sawyer, G.M., 2006. Rapid FTIR sensing of volcanic gases released by Strombolian explosions at Yasur volcano, Vanuatu. Appl. Phys. B 85, 453–460. http://dx.doi.org/10.1007/s00340-006-2353-4.

Peltier, A., Finizola, A., Douillet, G.A., Brothelande, E., Garaebiti, E., 2012. Structure of an active volcano associated with a resurgent block inferred from thermal mapping: The Yasur–Yenkahe volcanic complex (Vanuatu). J. Volcanol. Geotherm. Res. 243–244, 59–68.

Petersen, T., De Angelis, S., Tytgat, G., McNutt, S., 2006. Local infrasound observations of large ash explosions at Augustine Volcano, Alaska, during January 11-28, 2006. Geophys. Res. Lett. 33. http://dx.doi.org/10.1029/2006GL026491 (L12303).

Ripepe, M., Marchetti, E., 2002. Array tracking of infrasonic sources at Stromboli volcano. Geophys. Res. Lett. 29 (22), 2076. http://dx.doi.org/10.1029/2002GL015452.

Ripepe, M., Poggi, P., Braun, Gordeev, E., 1996. Infrasonic waves and volcanic tremor at Stromboli. Geophys. Res. Lett. 23, 181–184.

Ripepe, M., Marchetti, E., Ulivieri, G., 2007. Infrasonic monitoring at Stromboli volcano during the 2003 effusive eruption: insights on the explosive and degassing process of an open conduit system. J. Geophys. Res. 112. http://dx.doi.org/10.1029/2006JB004613.

Ripepe, M., Delle Donne, D., Harris, A., Marchetti, E., Ulivieri, G., 2008. Dynamics of Strombolian Activity. In: Calvari, S. (Ed.), The Stromboli Volcano: An Integrated Study of the 2002–2003 Eruption. Am. Geophys. Union, pp. 39–48.

Taddeucci, J., Sesterhenn, J., Scarlato, P., Stampka, K., Del Bello, E., Pena Fernandez, J.J., Gaudin, D., 2014. High speed imaging, acoustic features, and aeroacoustic computations of jet noise from Strombolian (and Vulcanian) explosions. Geophys. Res. Lett. 41, 3096–3102. http://dx.doi.org/10.1002/2014GL059925.

Wilson, L., Head, J.W., 1981. Ascent and eruption of basaltic magma on the Earth and Moon. J. Geophys. Res. 86, 2971–3001.

Zielinski, C., Vergniolle, S., Bani, P., Lardy, M., Le Pichon, A., Ponceau, D., Gallois, F., Herry, P., Todman, S., Garaeibiti, E., 2010. The potential of continuous near-field recording of infrasound produced by volcanoes in Vanuatu for probing the state of the atmosphere. EGU General Assembly 2010. Geophys. Res. Abstr. Vol. 12 (EGU2010-1055).